Probing the 4U 1624-490 Ionized Gas and Dust distribution along the LOS

Jingen Xiang[1], Julia. C. Lee[2] (Harvard University) and Michael. A. Nowak[3], Norbert S Schulz[4] (MIT)
1. jxiang@cfa.harvard.edu 2. jclee@cfa.harvard.edu 3. mnowak@space.mit.edu 4. nss@space.mit.edu

Abstract

We present results based on our 76 ks Chandra HETGS observation of the "Big Dipper" 4U 1624-490. Specifically, we discuss how the line profiles change with phase in the context of the geometry of the system as well as changes in plasma conditions over the 4U 1624-490 binary orbit. In addition, we will show how we have used the associated dust scattering halo to derive a geometric distance of ~15 kpc to this binary, as well as assess location, uniformity and density of ISM dust grains along the line of sight to this source.

§1. Introduction

1. Source – 4U 1624-490: A Low Mass X-ray Binary (LMXB), also known as "The Big Dipper" because of its ~3 hr dip duration, long orbital period of ~21 hr and large obscuration covering ~90% of the compact object.

2. Dip: Thought to be due to occultations of the central source by gas from the accretions disk rim.

3. Observation: The source was observed with the *Chandra* High Energy Transmission Grating Spectrometer (HETGS) in timed graded mode from 2004 June 4 06:26:06 to 03:46:17 (ObsID: 4559) for 76 ks, covering one binary orbit.

§ 2. Distance to 4U 1624-490

Photons which have been scattered by dust along the LOS travel longer distances than the unscattered one (see Fig.1). The delay time *dt* is given by

$$dt = 1.15\,h(D/1\,kpc)(\theta/1\,arcmin)^2\frac{x}{1-x}$$

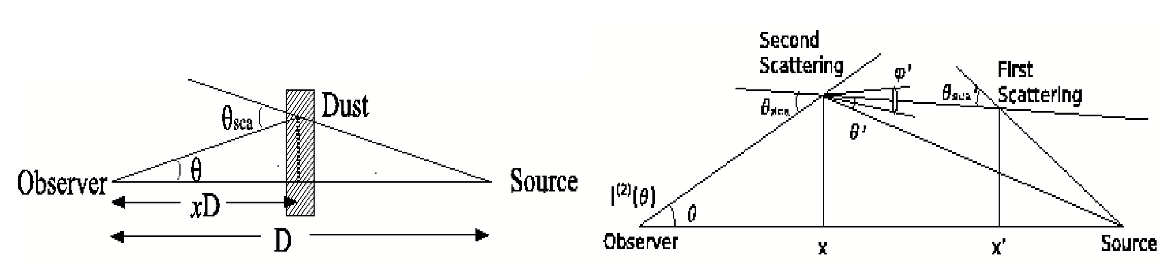

Fig 1. Geometry of the X-ray-scattering process for single (left) and double (right) scattering.

Therefore the halo and binary light curves can be used to determine the distance to the point source (Fig 2).

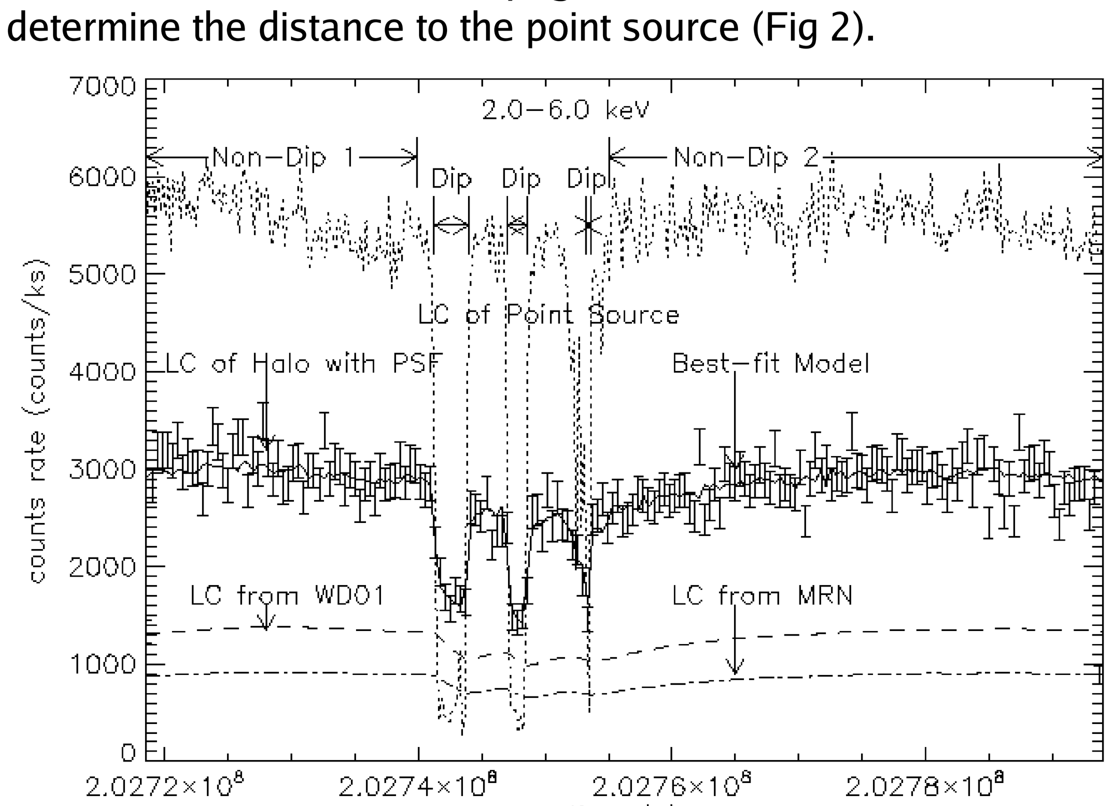

Fig. 2. We were able to derive a distance $D_{4U1624-490}=15.0^{+2.9}_{-2.6}$ kpc to 4U 1624-490 by fitting to the halo light curve surrounding it in combination with the measured delay time in halo light curve response to source flux behavior.

§ 3. Varying Dust Distribution

X-ray halo properties tightly depend upon the relative distances to the scatterings by the dust grains. We thus were able to use geometric arguments to study halo profiles and distinguish the location of dust clouds close to the X-ray binary (sharp, narrow halos) from those close to us (flat, wide halos), and thereby determine their spatial distribution. We determined the dust distribution along the line-of-sight to the neutron star binary 4U1624-490, and have found that it is largely clumped in the spiral arms of our MW galaxy. These spiral arms have different particle density distributions than the intervening Galactic regions (See Fig 3).

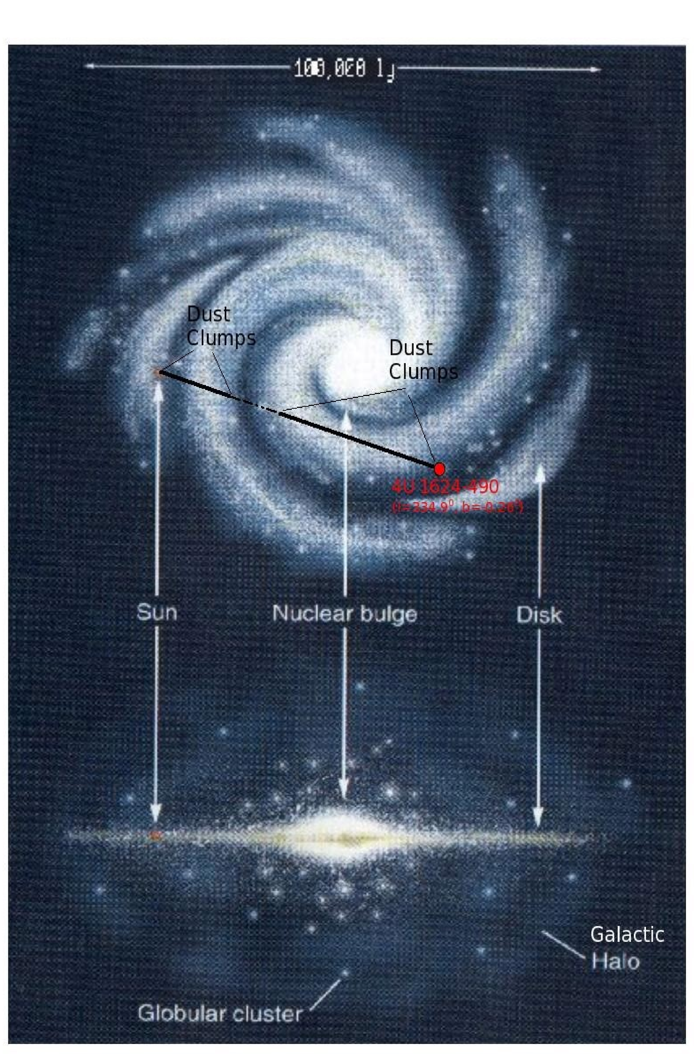

Fig. 3. The location of 4U 1624-490 and the spatial distribution of dust along the LOS

The X-ray halo radial profiles are shown in Fig 4.

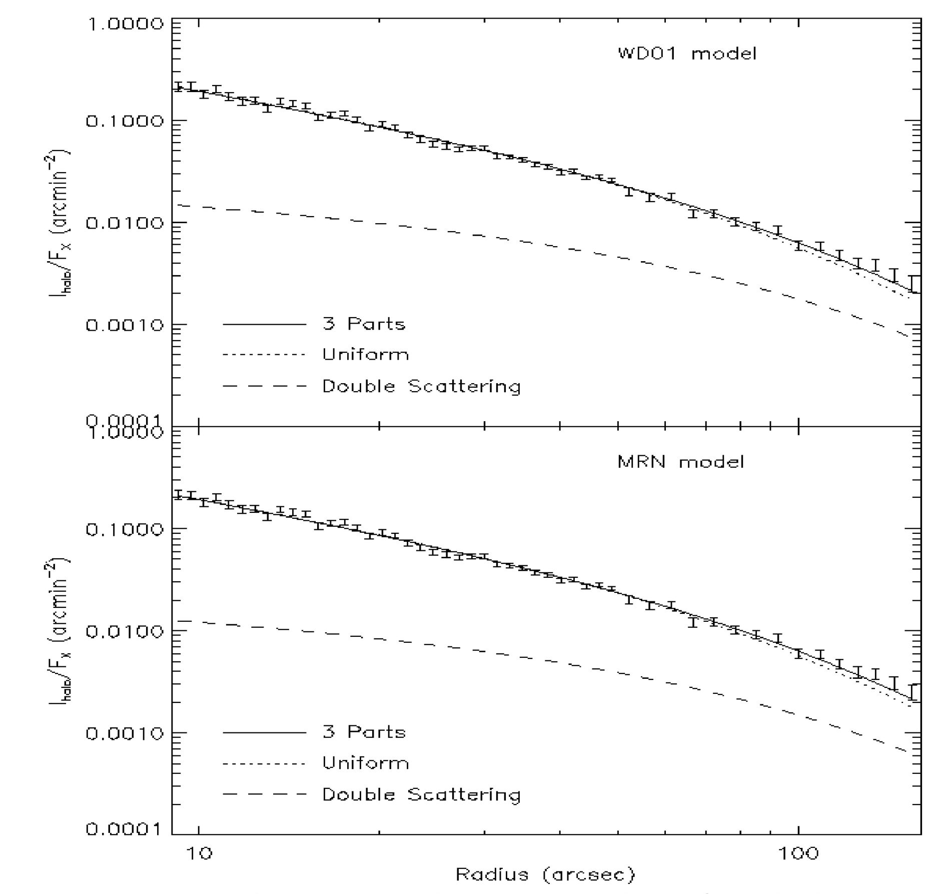

Fig 4. X-ray halos observed at 2.0—6.0 keV, fit with dust grains model WD01 and (top) MRN77 (bottom). It is clear that non-uniform dust distibution is preferred.

§ 4. Light Curves Reveal Large Obscuration

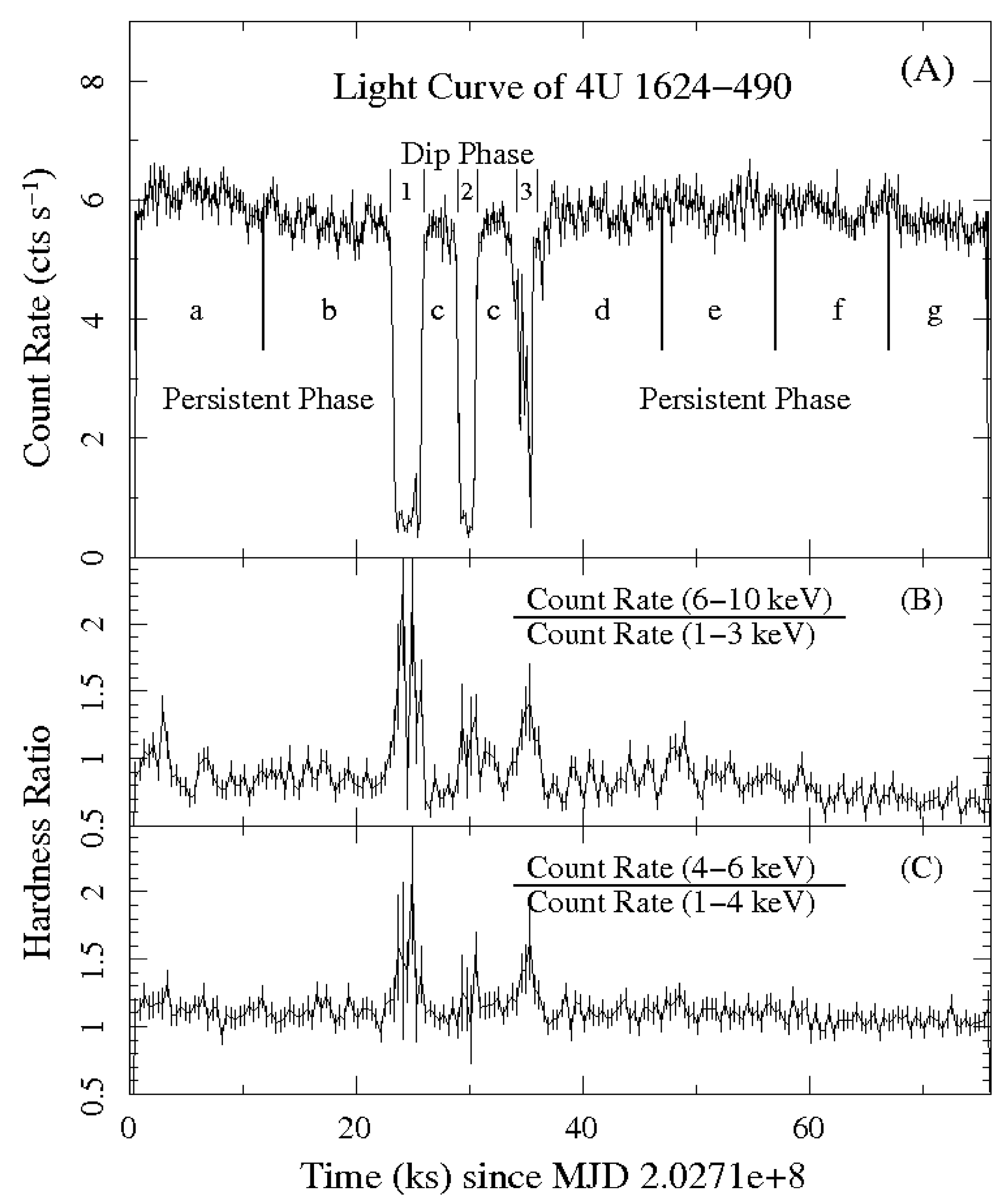

Fig. 5. (A) First-order HEG+MEG light curve of 4U 1624-490 between 1.0-10.0 keV, covering one orbital phase and associated hardness ratio (B, C). Hardness ratios are seen to increase during the dipping phases.

§ 5. Evolving Line Profiles with Phase

While the broadband continuum spectrum changes little over the duration of the orbital phase, the ionized H-like and He-like Fe lines show variability in both flux and wavelength (Fig. 6 and 7). The green lines indicate the laboratory wavelengths of Fe XXV (1.850 Å) and Fe XXVI (1.778 Å) resonant absorption.

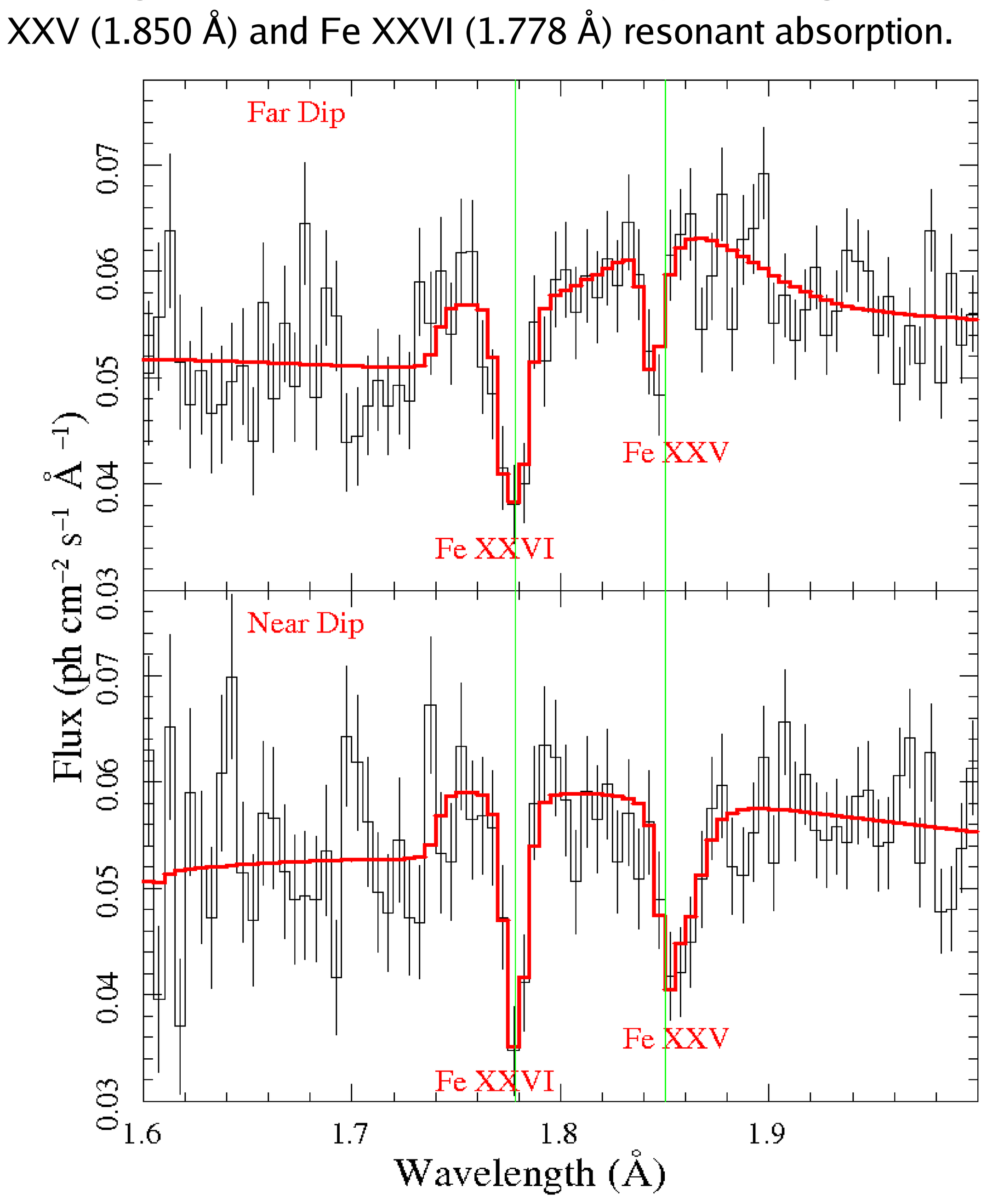

Fig.6. Best fit ionized absorber models (red) overplotted on the HEG 1[st] order far dip (top) and near dip (bottom) spectra.

Based on these spectra, we determine a radius for a hot (T~3×10^6 K) component of plasma to be r~3×10^{10} cm (possibly ADC) and a colder (T~10^6 K) component to be r~10^{11} cm (possibly the AD truncation radius). A toy model about the location of two temperature ionized gas is shown in Fig 8.

We also divided the persistent spectrum into ~7 parts of ~10 ksec duration (Fig. 6). The Fe XXV and Fe XXVI line fluxes and profiles clearly evolve with phase.

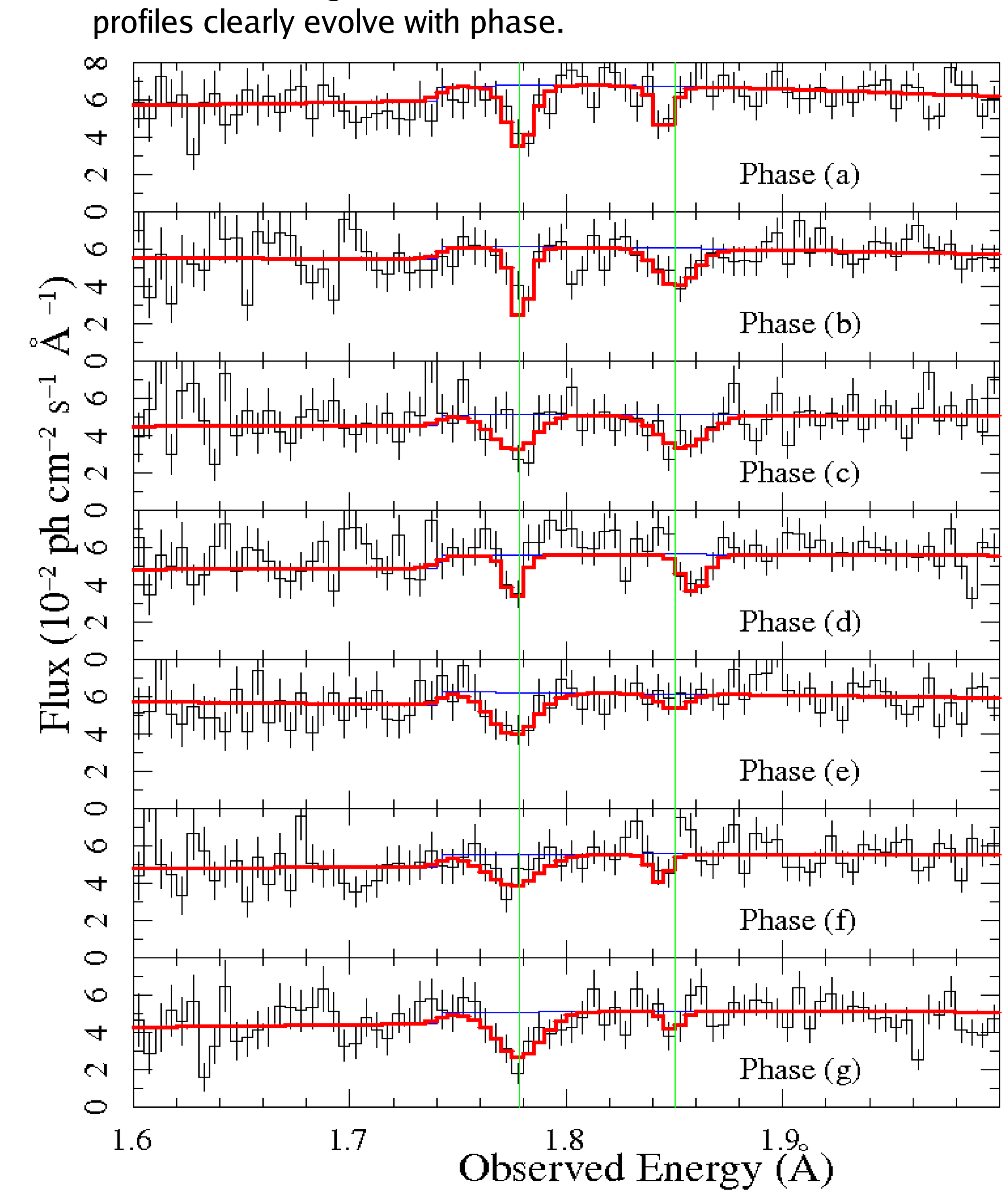

Fig. 7. The evolution of Fe XXV and Fe XXVI lines.

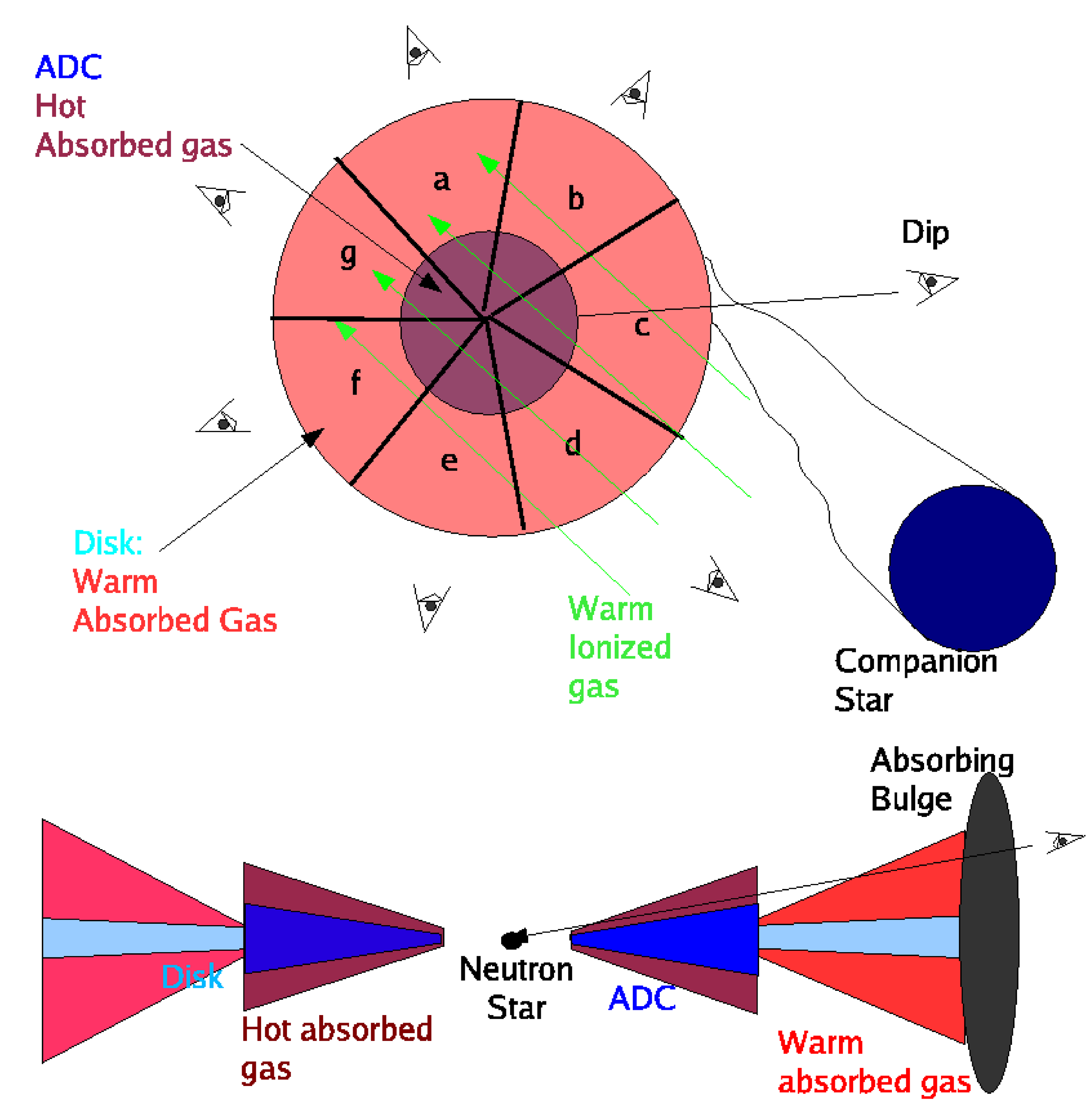

Fig. 8 Possible geometry showing how the location of the two temperature ionized gas evolves with phase.

Conclusion:

(1) Xiang, Lee & Nowak 2007:

• We determine a distance $D_{4U1624-490}=15.0^{+2.9}_{-2.6}$ kpc to 4U 1624-490 based on scattering halo studies [7].

• Varying dust distribution ***does*** affect the derived column densities along the LOS to 4U 1624-490. A simple estimate based on our halo fits imply the hydrogen particle density in the spiral arms is n~1.6 cm^{-3} and the one between two spiral arms n<0.3 cm^{-3}.

(4) Xiang, Lee & Nowak in final prep:

• Evolving iron absorption line profiles with orbital phase during the persistent phase of 4U 1624-490 are observed.

• The evolution of these lines can be modelled using the "XSTAR" photoionization code which places the location of the gas in the region of the ADC and disk.

Main References:

[1]. Caswell J. L. & Haynes F. F. 1987, A&A, 171, 261
[2]. Church M., J. & Balucinska-Church, M, 2004, MNRAS, 348, 955
[3]. Mathis, J. S., Rumpl,W. & Nordsieck, K. H. 1977, ApJ, 217, 425 (MRN)
[4]. Mathis, J. S. & Lee, C. W. 1991, ApJ, 376, 490
[5]. Predehl, P., Burwitz, V., Paerels, F., & TrÜmper, J. 2000, A&A, 357, L25
[6]. Weingartner, J. C. & Draine, B. T. 2001, ApJ, 548, 296 (WD01)
[7]. Xiang, J., Lee J. C., & Nowak, M., 2007, ApJ, 660, 1309